# High-precision half-life measurements for the superallowed Fermi $\beta^+$ emitter $^{14}$O

A. T. Laffoley,[1,*] C. E. Svensson,[1] C. Andreoiu,[2] R. A. E. Austin,[3] G. C. Ball,[4] B. Blank,[5] H. Bouzomita,[6] D. S. Cross,[2] A. Diaz Varela,[1] R. Dunlop,[1] P. Finlay,[1,†] A. B. Garnsworthy,[4] P. E. Garrett,[1] J. Giovinazzo,[5] G. F. Grinyer,[6] G. Hackman,[4] B. Hadinia,[1] D. S. Jamieson,[1] S. Ketelhut,[4] K. G. Leach,[1,‡] J. R. Leslie,[7] E. Tardiff,[4,§] J. C. Thomas,[6] and C. Unsworth[4]

[1]*Department of Physics, University of Guelph, Guelph, Ontario N1G 2W1, Canada*

[2]*Department of Chemistry, Simon Fraser University, Burnaby, British Colombia V5A 1S6, Canada*

[3]*Department of Astronomy and Physics, Saint Mary's University, Halifax, Nova Scotia B3H 3C3, Canada*

[4]*TRIUMF, 4004 Wesbrook Mall, Vancouver, British Columbia V6T 2A3, Canada*

[5]*Centre d'Etudes Nucléaires de Bordeaux Gradignan-Université, Bordeaux 1-UMR 5797 CNRS/IN2P3, Chemin du Solarium, BP 120, F-33175 Gradignan Cedex, France*

[6]*Grand Accélérateur National d'Ions Lourds (GANIL), CEA/DSM-CNRS/IN2P3, Boulevard Henri Becquerel, 14076 Caen, France*

[7]*Department of Physics, Queens University, Kingston, Ontario K7L 3N6, Canada*

(Received 1 May 2013; published 1 July 2013)

The half-life of the superallowed Fermi $\beta^+$ emitter $^{14}$O has been determined via simultaneous direct $\beta$ and $\gamma$ counting experiments at TRIUMF's Isotope Separator and Accelerator (ISAC) facility. A $\gamma$-ray counting measurement was performed by detecting the 2312.6-keV $\gamma$ rays emitted from an excited state of the daughter $^{14}$N following the implantation of samples at the center of the $8\pi$ $\gamma$-ray spectrometer, a spherical array of 20 high-purity germanium (HPGe) detectors. A simultaneous $\beta$ counting experiment was performed using a fast plastic scintillator positioned behind the implantation site with a solid angle coverage of ∼20%. The results, $T_{1/2}(\beta) = 70.610 \pm 0.030$ s and $T_{1/2}(\gamma) = 70.632 \pm 0.094$ s, form a consistent set and, together with eight previous measurements, establish a new average for the $^{14}$O half-life of $T_{1/2} = 70.619 \pm 0.011$ s with a reduced $\chi^2$ of 0.99.

DOI: 10.1103/PhysRevC.88.015501 PACS number(s): 23.40.−s, 21.10.Tg, 24.80.+y, 27.20.+n

## I. INTRODUCTION

High-precision measurements of the $\beta$ decay $ft$ values for superallowed Fermi $\beta$ transitions between nuclear analog states of spin $J^\pi = 0^+$ and isospin $T = 1$ provide demanding, and fundamental, tests of the properties of the electroweak interaction [1]. The $ft$ value that characterizes any $\beta$ transition depends on three measurable quantities: the total transition energy, or $Q$ value, required to determine the statistical rate function $f$; the half-life $T_{1/2}$ of the parent; and the branching ratio $R$ to the particular state of interest. In the case of superallowed Fermi $\beta$ emitters, transitions between isobaric analog states directly probe the weak vector current and can also be used to constrain the presence of induced or fundamental scalar currents in $\beta$ decay. Measurements of these $ft$ values have been used to validate the conserved vector current (CVC) hypothesis to better than 2 parts in $10^4$ and provide the most precise determination of $V_{ud}$, by far the most precisely measured element of the Cabibbo-Kobayashi-Maskawa (CKM) quark mixing matrix [2].

The presence of a fundamental scalar interaction (or one induced by the vector current) would affect the corrected $ft$ values, denoted $\mathcal{F}t$, for the superallowed $\beta$ emitters [3]. The $\mathcal{F}t$ values would cease to be constant as a function of $Z$, and for maximally parity-violating scalar interactions, the $\mathcal{F}t$ values would contain an additional term approximately proportional to the average inverse decay energy of the $\beta^+$ transition, $\langle 1/Q \rangle$. The largest deviations of the $\mathcal{F}t$ values from a constant would thus occur in the lightest of the superallowed $\beta^+$ emitters, $^{10}$C and $^{14}$O, for which the decay $Q$ values are the smallest. The $ft$ values for these isotopes are thus crucial for setting limits on the existence of scalar weak interactions.

The precision of the $\mathcal{F}t$ value for $^{14}$O is currently limited, almost in equal parts, by the precision thus far achieved experimentally in the $Q$ value, the branching ratio, and the nuclear-structure-dependent theoretical corrections ($\delta_C - \delta_{NS}$), each of which contributes a fractional uncertainty of 5, 6, and 5 parts in $10^4$, respectively [1].

The $Q$ value, 2831.24(23) keV, for $^{14}$O superallowed decay was last deduced in 2003 using a $(p, n)$ reaction [4], and among the 13 most precisely measured $ft$ values for superallowed emitters, only $^{14}$O has not yet had its mass measured with a Penning trap mass spectrometer. A Penning trap mass measurement for $^{14}$O is planned with TRIUMF's Ion Trap for Atomic and Nuclear Science (TITAN) [5] in 2013 and a significant improvement in the $^{14}$O $Q$ value precision is expected in the near future.

There are significant experimental challenges in measuring the superallowed branching ratio for $^{14}$O decay, and the current uncertainty associated with the superallowed branch is a direct result of the uncertainty attributed to the weak branch (∼0.6%) populating the $1^+$ ground state of $^{14}$N via an allowed Gamow-Teller transition. All previous branching ratio measurements were performed over 40 years ago [6–8] and were recently reanalyzed in Ref. [9]. The adopted superallowed branching

*alaffole@uoguelph.ca

†Present address: Instituut voor Kern-en Stralingsfysica, K.U. Leuven, Celestijnenlaan 200D, B-3001 Leuven, Belgium.

‡Present address: TRIUMF, 4004 Wesbrook Mall, Vancouver, British Columbia V6T 2A3, Canada.

§Present address: Department of Physics, Harvard University, Cambridge, Massachusetts 02138, USA.

 

ratio of 99.374(68)% is currently limited by the inconsistencies between these measurements that prompt Hardy and Towner, in their world survey of superallowed data [1], to apply a scale factor of 3.7 to the statistical uncertainty. Reducing this uncertainty poses a complex experimental challenge but is currently being addressed through techniques to measure high-precision branching ratios for the $T_z = -1$ superallowed emitters [10,11] with aims of potentially discriminating between theoretical model predictions of isospin symmetry breaking.

Finally, the dominant theoretical uncertainty is that of the nuclear-structure-dependent part of the radiative correction, $\delta_{NS}$ [12]. Discriminating between the various theoretical models has been a cornerstone of the investigation of superallowed emitters and is a major goal of current research.

Although a weighted average of the eight previous precision measurements of the $^{14}$O half-life yields 70.620(12) s, a result that is precise to $\pm 0.019\%$ and currently makes a minority contribution to the quoted precision of the $^{14}$O superallowed $\mathcal{F}t$ value, there is cause to question the *accuracy* of this average $T_{1/2}$ value. Based on the $\chi^2/\nu$ of 1.26, these results form an inconsistent data set and prompt Hardy and Towner in their world survey of superallowed data [1] to apply a scale factor of 1.2 to the statistical uncertainty in the $^{14}$O half-life and adopt a value of $70.620 \pm 0.015$ s. Furthermore, among these eight previous measurements it should be noted that there are two methods for measuring the half-life of $^{14}$O; one can either directly count the $\beta$ particles or measure the $\gamma$ activity since, with a branching ratio of 99.4%, $^{14}$O decays to an excited state of its daughter $^{14}$N which then emits a 2312.6-keV $\gamma$ ray. Averaging the experiments that detected 2312.6-keV $\gamma$ rays yields an average value of $T_{1/2}(\gamma) = 70.598(17)$ s while the two direct $\beta$ counting measurements of Refs. [13,14] yield $T_{1/2}(\beta) = 70.648(19)$ s, results that have a $\chi^2/\nu = 3.85$ if considered as two independent techniques for the measurement of the same quantity. Choosing either of these methods to be correct would shift the $^{14}$O $\mathcal{F}t$ value, one of the most precisely quoted of all of the superallowed decays, by $0.5\sigma$. This would have direct implications on the overall value deduced for $V_{ud}$, the test of CKM unitarity, and the present constraint on the existence of a fundamental or induced scalar interaction in the minimal electroweak Standard Model.

It is this half-life discrepancy, together with the expectation of significant improvement in the experimental $Q$ value and branching ratio measurements in the near future, that motivated the simultaneous high-precision $\beta$ and $\gamma$ counting $^{14}$O half-life measurements reported here.

## II. EXPERIMENT

The experiment was performed at the Isoptope Separator and Accelerator (ISAC) facility at TRIUMF, Canada's national laboratory for particle and nuclear physics. A beam of 500-MeV protons impinged on a SiC target, causing spallation reactions whose products diffused from the target and were ionized using a Forced Electron Beam Ion Arc Discharge (FEBIAD) ion source. A mass separator was used to select a beam of $A = 26$ products, including the primary beam of carbon monoxide ($^{12}$C$^{14}$O) molecules, as well as contaminants of $^{26}$Na, $^{26}$Al$^g$, and $^{26}$Al$^m$.

The beam was implanted, under vacuum, at the center of the $8\pi$ spectrometer [15] onto a movable mylar-backed aluminum-tape transport system for 3 min, or approximately 2.5 $^{14}$O half-lives, prior to being deflected before the mass separator two floors below the experimental hall. The sample collected on the tape was then allowed to decay for 23 min, or approximately 20 $^{14}$O half-lives. This constituted a single run, at which time the tape was moved outside the array behind a thick lead wall to remove any long-lived contaminants ($^{26}$Al$^g$) from the array, and the cycle was repeated. It is known that the diffusion of $^{14}$O implanted as CO can be an issue when using very thin aluminized mylar tape. However, the $8\pi$ system uses a tape consisting of a 40-$\mu$m-thick layer of aluminum on a backing of mylar to avoid this potential diffusion problem. A total of 102 runs were taken during the experiment. The $8\pi$ $\gamma$-ray spectrometer, a spherically symmetric array of 20 high-purity germanium (HPGe) detectors each equipped with a bismuth germinate (BGO) Compton-suppression shield; the upstream half (10 plastic scintillators) of the Scintillating Electron-Positron Tagging Array (SCEPTAR) [16]; and the Zero-Degree Scintillator (ZDS), a fast plastic scintillating detector positioned at zero degrees relative to the beam axis and directly behind the thin aluminized mylar tape on which the beam was implanted, were used to collect data. The ZDS is a 1-mm-thick BC-422Q ultrafast timing plastic scintillator by Saint-Gobain coupled to a H6522 Hamamatsu photomultiplier tube, and the solid angle subtended by the ZDS was approximately $1\pi$. Data were collected during both the implantation and decay stages of each run.

The $\gamma$-ray singles events were recorded and time stamped with a Stanford Research Systems 10 MHz $\pm$ 0.1 Hz temperature-stabilized precision laboratory clock providing the time standard. The $8\pi$ data-acquisition system provides a pile-up indicator for each HPGe detector using an inhibit signal from the Ortec 572 spectroscopy amplifier into a time-to-digital converter (TDC). A variable (measured event by event) or fixed nonextendible dead time of the entire system per event as well as Compton suppression can be selected in software. Compton suppression was not used in this high-precision half-life determination due to the potential bias from rate-dependent false-veto events. More details of the $\gamma$-ray detection system used for half-life measurements is provided in Ref. [17]. The nonextendible dead time of the data-acquisition system, as well as the shaping times of the HPGe spectroscopy amplifiers, were varied throughout the experiment in order to investigate possible systematic effects. Data were collected with combinations of three dead-time settings (variable, fixed 30 $\mu$s, and fixed 50 $\mu$s) and three HPGe spectroscopy amplifier shaping times (0.5 $\mu$s, 1.0 $\mu$s, and 2.0 $\mu$s).

The signals from $\beta$ particles detected in the ZDS were fanned out into five data streams and multiscaled into bins of 6-s duration using five independent channels of a VME-based multichannel scaler (MCS). Several fixed and nonextendible dead times were chosen that were much longer than the total series dead time of the system. These were applied to each MCS stream using LeCroy 222N nonretriggerable gate-and-delay generators. The dead times applied to the five MCS

channels were approximately 2, 5, 10, 20, and 30 $\mu$s (the measured dead-time values are discussed below in Sec. III A).

The current of the primary proton beam was increased throughout the experiment in steps from 50 to 60, 65, and finally 70 $\mu$A in order to provide a more intense beam to the detector system. Approximately halfway through the experiment the current of the FEBIAD ion source was also increased in order to increase the intensity of $^{14}$O by a factor of ~4. After the FEBIAD tune and with a proton beam current of 70 $\mu$A the beam was delivered to the tape-transport system with a rate of approximately $3.5 \times 10^4$ $^{14}$O/s, $2 \times 10^5$ $^{26}$Na/s, and $3 \times 10^3$ $^{26}$Al$^m$/s, compared to $3.5 \times 10^3$ $^{14}$O/s delivered before the FEBIAD tune and with a proton beam current of 50 $\mu$A. The effects of these changes in experimental conditions are explored as potential systematic effects in Secs. III A and IV A.

## III. $\beta$ COUNTING RESULTS

Following dead-time corrections [17,18], the data were fit using a maximum-likelihood technique described in previous works [17–20]. The fitting routine included a component for the $^{14}$O activity, the $^{26}$Na activity, the $^{26}$Al$^m$ activity, and a constant background. With a half-life of $7.17(24) \times 10^5$ years [21] the contaminant of $^{26}$Al$^g$ was treated as a constant activity on the time scale of a single run (23 min), thereby being included with the constant background. The fit was started at channel 41, two channels (12 s) after the beam was deflected, to ensure the beam was not being implanted on the tape for a fraction of the channel width, thus biasing the observed initial decay rate. The half-lives of both $^{26}$Na and $^{26}$Al$^m$ were fixed at their precisely determined values of 1.07128(25) s [18] and 6.34632(70) s [19], respectively. Effects of the small uncertainties in these contaminant half-lives are explored in detail in Sec. III A. A typical decay curve from a single run is presented in Fig. 1.

In order to explore rate-dependent and diffusive systematic effects, leading channels were removed from the analysis and the data were refit as a function of the starting channel number. In order to quantify the trends observed in these leading channel removal plots, which are composed not of independent points but rather highly correlated data, the following metric was defined:

$$M = \sum_{x=1}^{12} \mathrm{sgn}\big(T_{1/2}(x) - T_{1/2}(0)\big)\left[\frac{T_{1/2}(x) - T_{1/2}(0)}{\sigma_x}\right]^2,$$

where $x$ represents the number of leading channels removed (each channel has a duration of 6 s), $\sigma_x$ is the statistical error associated with the fit after removing $x$ leading channels, $\mathrm{sgn}(x)$ is the signum function, and the sum was computed over 12 channels representing more than one half-life of the $^{14}$O decay. This metric quantitatively identifies any runs that have significant rate-dependent trends in either direction and results in approximately zero for leading channel removal plots that gradually "oscillate" (because of point-by-point correlations of the data) about a mean central value. The results of this metric were used as a guide to indicate which leading channel removal plots should be further investigated, and the results are plotted in Fig. 2 for all 102 runs recorded during the experiment. Four runs were identified as having an anomalous rate dependence in their deduced half-lives and were removed from the final analysis. It is important to note that although all four anomalous runs had negative values of the leading channel removal metric $M$ (decreasing $T_{1/2}$ with removal of leading channels), the sign of $M$ is not correlated with the absolute value of $T_{1/2}$ at $x = 0$, as one of the runs had an above-average $T_{1/2}$ and three were below average.

The remaining 98 dead-time corrected runs were then summed before being fit in order to avoid the known bias resulting from averaging many $T_{1/2}$ measurements of lower statistics [20]. A summary of the half-lives from the individual runs is presented in Fig. 3(a) and the fitted, dead-time corrected summed (global) data set with residuals is presented in Fig. 4(a). When channels were systematically removed from the beginning of the data set, as presented in Fig. 5, no evidence for a change in half-life was observed, and we conclude that there is no systematic rate-dependent trend and that diffusion at these time scales can be considered negligible for the implanted $^{14}$O ions.

### A. Systematic uncertainties

The $\beta$ data stream was fanned into five separate and independent channels of a multichannel scaler module to bin the decay data, with a different fixed nonextendible dead time applied to each channel. The fixed dead times were measured to be 1.9818(37), 5.0041(41), 10.0042(38), 20.0109(60), and 29.9906(86) $\mu$s by the source-plus-pulser method [22]. The half-life of $^{14}$O as determined by each of these MCS data streams (labeled by their dead-times) was $T_{1/2}^{\mathrm{MCS2}} = 70.609 \pm 0.020$ s, $T_{1/2}^{\mathrm{MCS5}} = 70.609 \pm 0.020$ s,

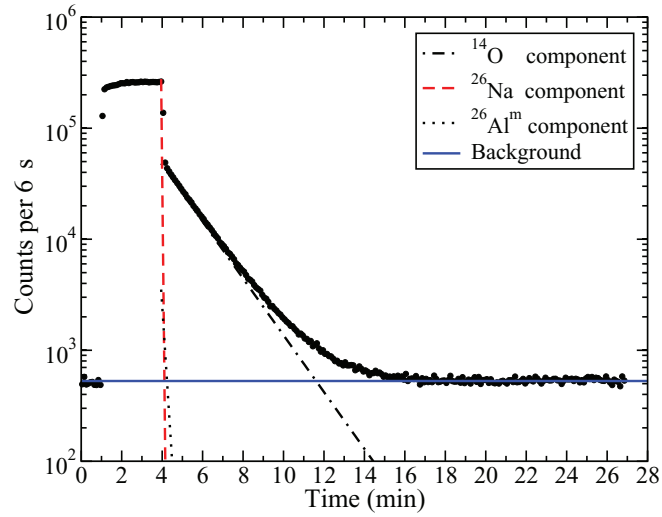


FIG. 1. (Color online) A sample of the dead-time-corrected $\beta$ data from a single MCS channel for a single run. The decay components are highlighted: the $^{14}$O (black, dot dashed line), the $^{26}$Na contamination (red online, dashed line), the $^{26}$Al$^m$ contamination (black, dotted line), and the background (blue online, solid line).

$T_{1/2}^{\mathrm{MCS10}} = 70.608 \pm 0.020$ s, $T_{1/2}^{\mathrm{MCS20}} = 70.609 \pm 0.020$ s, and $T_{1/2}^{\mathrm{MCS30}} = 70.615 \pm 0.020$ s. Because the scalers independently bin the same data, they are not independent measurements of the half-life of $^{14}$O but provide a consistency check of the dead-time corrections. Since all five values are consistent, the unweighted average, $T_{1/2} = 70.610 \pm 0.020$ s, is adopted as the half-life of $^{14}$O from these measurements.

To further test for potential systematic uncertainties, runs were grouped according to two additional experimental conditions: the beam current of the primary proton beam [50 $\mu$A (5 runs), 60 $\mu$A (21 runs), 65 $\mu$A (6 runs), 70 $\mu$A (66 runs)], which yield a reduced $\chi^2$ of 0.42, and whether the run came before (71 runs) or after (27 runs) the ion source tune, which yield a reduced $\chi^2$ of 0.86 as summarized in Fig. 6. Both of these groupings yield a reduced $\chi^2$ value below 1. However, as noted in Fig. 3(a), the half-lives determined in the 98 individual runs yield a reduced $\chi^2$ of 2.27. Although the large $\chi^2/\nu$ in the $\beta$ data recorded with the ZDS could not be correlated systematically with any known experimental parameter, to be conservative we adopt the method of the Particle Data Group [23] and inflate the statistical uncertainty of 0.020 s by the square root of 2.27 to estimate the potential contribution to the overall uncertainty from an unidentified systematic effect, leading to an overall uncertainty of 0.030 s. As a final consistency check, the measured dead times, as well as the fixed half-lives of the $^{26}$Na and $^{26}$Al$^m$ contaminants, were varied within their $\pm 1\sigma$ values and the data were refit. These variations contributed negligibly to the uncertainty of the deduced $^{14}$O half-life, at the $5 \times 10^{-4}$ and $<10^{-5}$ levels, respectively.

Assuming that the statistical and systematic uncertainties are independent quantities and can be combined in quadrature to obtain the overall uncertainty, the half-life of $^{14}$O determined from direct $\beta$ counting in this work is $T_{1/2}(\beta) = 70.610 \pm 0.020_{\mathrm{stat.}} \pm 0.023_{\mathrm{syst.}}$ s. The precision of this result is comparable to the best previous individual measurement of the $^{14}$O half-life and is in good agreement with the eight previous measurements (see Sec. IV A below).

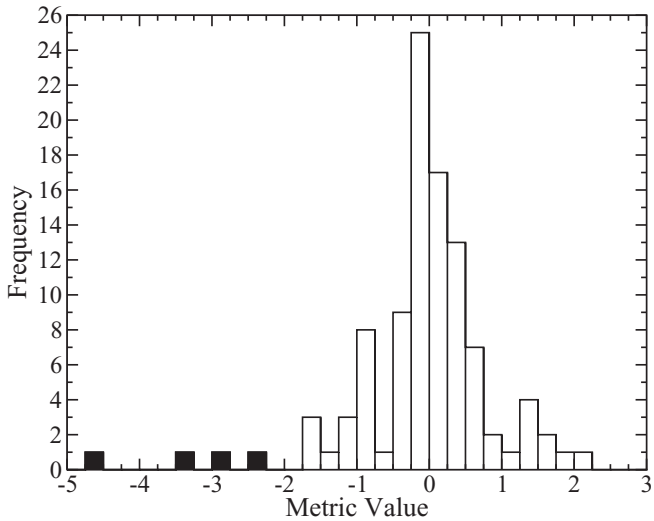


FIG. 2. The results of the leading channel removal metric as applied to the 102 runs for the $\beta$ data. Highlighted are the four runs with leading channel removal plots that were deemed anomalous and were removed from the final analysis of the $^{14}$O half-life. Note that the metric value is not correlated with the $T_{1/2}$ value for the excluded runs.

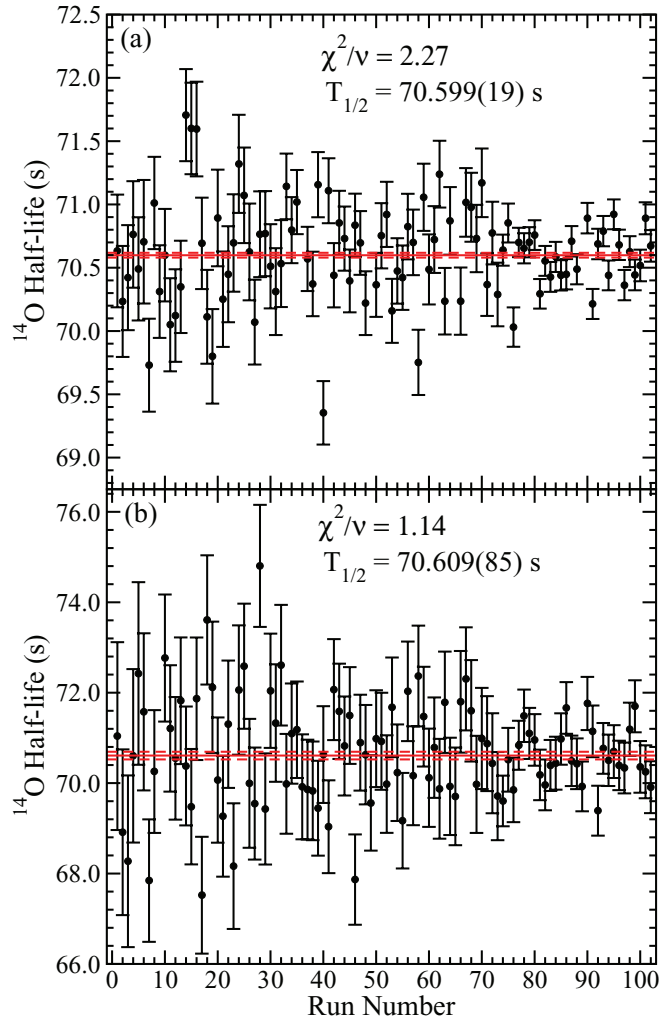


FIG. 3. (Color online) (a) Half-life vs run number obtained through $\beta$ counting with the ZDS. A weighted average was performed on this set, and the result is shown by the solid line and the $1\sigma$ uncertainties are shown by dashed lines. By averaging, rather than summing and then fitting, a small bias is introduced due to the lower statistics in each run [20]. The reduced $\chi^2$ obtained when averaging these values was $\chi^2/\nu = 2.27$ and is discussed in Sec. III. (b) Half-life vs run number obtained from the $\gamma$-ray measurements. A weighted average was performed on this set, and the result is indicated by the solid line and the $1\sigma$ uncertainties are shown by dashed lines.

## IV. $\gamma$ COUNTING RESULTS

The $^{14}$O half-life was also determined simultaneously by detecting 2312.6-keV $\gamma$ rays, which follow the superallowed decay of $^{14}$O and connect the excited analog $0^+$ state to the

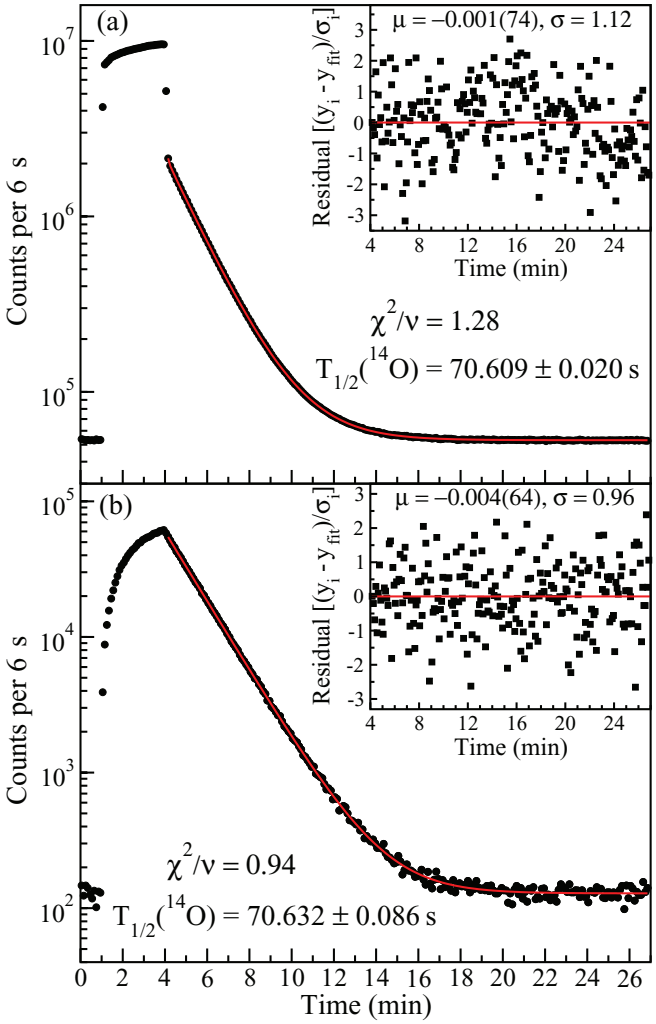


FIG. 4. (Color online) (a) Dead-time corrected activity curve of the summed (global) data from the $\beta$ counting experiment with the residuals (inset). These data represent the sum of the 98 good runs, with the data taken from the MCS data stream with 2-$\mu$s fixed dead time applied. (b) The dead-time and pile-up corrected activity curve of the summed (global) data from the $\gamma$-ray measurements with the residuals (inset). These data correspond to the 101 good runs with their appropriate $\gamma$-ray energy gates applied. The difference in relative contaminant intensities between the $\beta$ and $\gamma$ techniques can be clearly seen in the implantation grow-in behaviors between these two plots.

$1^+$ ground state in the daughter $^{14}$N [24]. The $\gamma$-ray spectrum recorded for a subset of these runs (40 in total) that were collected with a 2-$\mu$s HPGe spectroscopy amplifier shaping time is presented in Fig. 7.

A single run was removed from the final $\gamma$ analysis due to a data writing error in the $\gamma$-ray data stream. Thus, a total of 101 runs were used in the $\gamma$-ray analysis. Each was dead-time and pile-up corrected [17,25,26] before being fit. For this experiment, average pile-up corrections were applied where the averaging was performed across those runs with both the same shaping time (0.5/1/2 $\mu$s) and the same ion source tune (pre-/post-tune). These corrections were small, with a maximum pile-up probability of only 0.23% occurring at $t = 0$ for the "post-tune" (highest rate) data with the largest (2 $\mu$s)

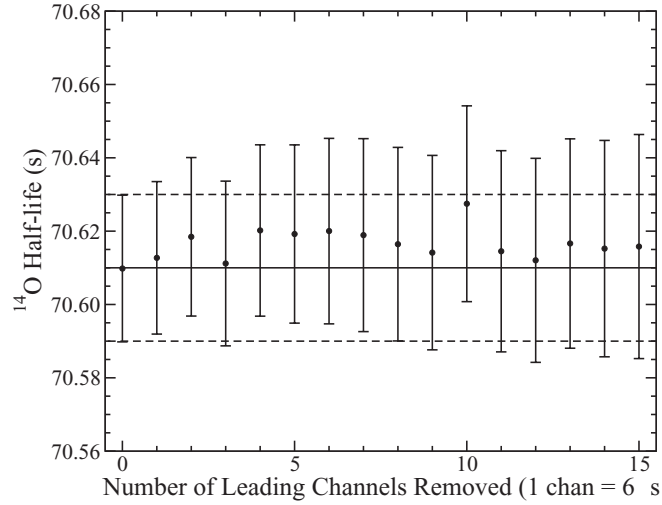


FIG. 5. Leading channel removal plot of the summed (global) data (all 98 runs) for the $\beta$ counting data. Each data point has been averaged over the five MCS channels (i.e., dead times) used. The half-life obtained in this work is overlaid for comparison. This plot confirms that diffusion of $^{14}$O is negligible with the thick aluminized mylar tape used in this experiment.

shaping time. Following the $\beta$ decay of $^{26}$Al$^m$, no known $\gamma$ radiation is produced [27] and the bremsstrahlung contribution at 2312.6 keV from the $^{26}$Al$^m$ decay positrons, with $\beta$ endpoint energy of 3210.7 keV, is also very small, so the activity due to $^{26}$Al$^m$ decay in the 2312.6-keV $\gamma$-ray window was entirely negligible. As a consistency check, the activity of $^{26}$Al$^m$ was also included in the fitting procedure as a free parameter but the activity derived from the fit was consistent with zero and was fixed to zero in the final analysis. The same fit function and

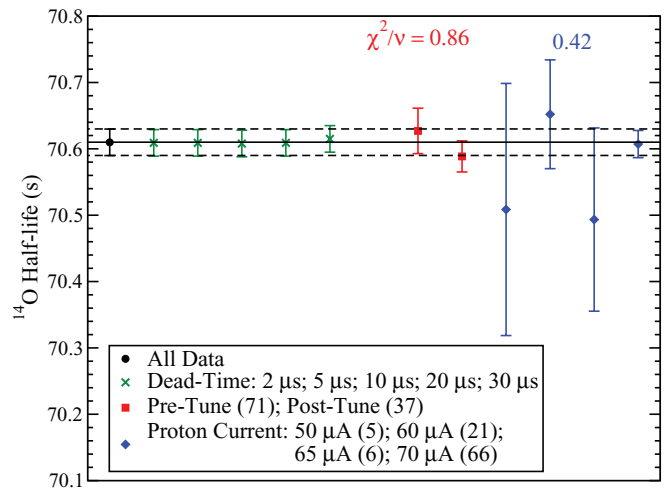


FIG. 6. (Color online) Half-life measurements of $^{14}$O grouped according to experimental parameters using the ZDS for $\beta$ detection. The numbers in parentheses indicate the number of runs corresponding to each setting. See text for details. The half-life as determined from each of the MCS channels (x's, green online), which correspond to different dead times, are not independent data sets and so no $\chi^2$ is calculated. The half-life determination via direct $\beta$ counting corresponds to the unweighted average of these five measurements.

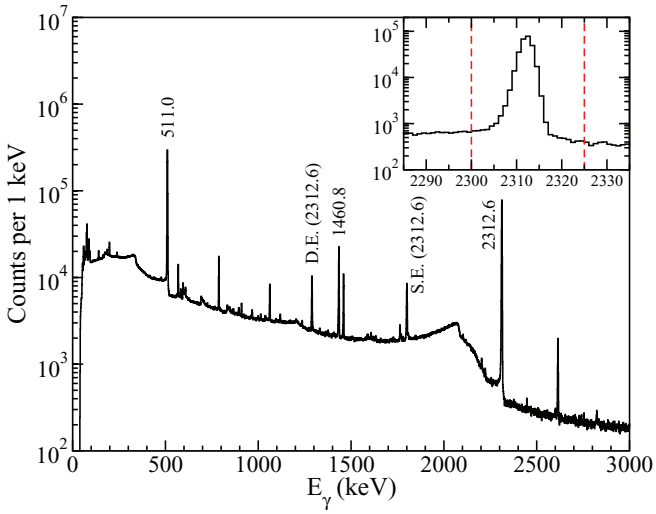


FIG. 7. (Color online) $\gamma$-ray singles spectrum for the 40 runs with 2-$\mu$s HPGe spectroscopy amplifier shaping time. It should be noted that this spectra shows the $\gamma$ rays detected >12 s after implantation finished (where the $T_{1/2}$ fit began) so that the majority of the $^{26}$Na $\gamma$-ray contamination has already decayed. The inset highlights the region around the 2312.6-keV $\gamma$ ray of interest. Dashed lines (red online) indicate the energy gate used in the half-life analysis.

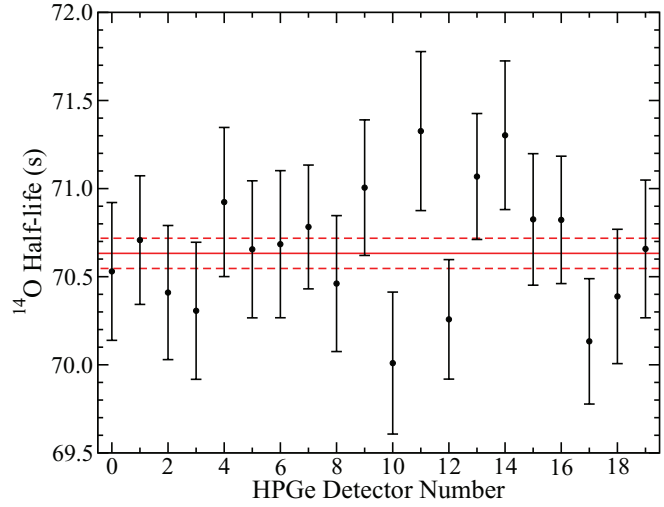


FIG. 8. (Color online) The $^{14}$O half-life as determined by each of the 20 HPGe detectors of the 8$\pi$ spectrometer [15]. These measurements form a consistent set and yield a reduced $\chi^2 = 0.88$. The half-life obtained in this work is overlaid for comparison.

fitting routine used in the $\beta$ analysis (see Sec. III) were used for the $\gamma$ analysis. The same metric was also applied to the leading channel removal plots as in the $\beta$ analysis (see Sec. III) and no anomalous runs were found. Each of the 101 runs were thus fit and treated as independent measurements, yielding a reduced $\chi^2$ of 1.14, as presented in Fig. 3(b). The 101 good runs were then summed and a global fit was performed to avoid the bias from averaging lower statistics $T_{1/2}$ measurements [20]. These summed data are presented in Fig. 4(b), yielding a $^{14}$O half-life of $T_{1/2}(\gamma) = 70.632 \pm 0.086$ s.

### A. Systematic uncertainties

To investigate potential systematic effects from the electronics, runs were grouped by electronic settings, summed, and subsequently fit. The three dead times used were variable (37 runs), 30-$\mu$s fixed (31 runs), and 50-$\mu$s fixed (33 runs), which yield a reduced $\chi^2$ of 1.15. The three shaping times used were 0.5 $\mu$s (14 runs), 1 $\mu$s (47 runs), and 2 $\mu$s (40 runs) and yield a reduced $\chi^2$ of 0.47. Similar to the $\beta$ analysis, an investigation of the proton beam current ($\chi^2/\nu = 1.18$) and the effects of the ion source tune ($\chi^2/\nu = 0.002$) were also investigated. Finally, the data recorded by the 20 HPGe detectors were analyzed independently and, as presented in Fig. 8, yield a reduced $\chi^2$ of 0.88. A summary of the results is presented in Fig. 9. Using the procedure adopted by the Particle Data Group, we inflate our statistical error (0.086 s) by the square root of the largest $\chi^2$, which came from the beam current grouping ($\chi^2/\nu = 1.18$), giving an estimate of the potential systematic error in the $\gamma$-ray measurement of 0.036 s.

An additional test of systematic contributions from the choice of the $\gamma$-ray energy gate used in the analysis was also explored. It would not have been unreasonable to have chosen an energy gate that was either one channel wider or narrower on each boundary, so the analysis was repeated for both of these cases to explore any effect of the gate choice. The runs were dead-time corrected, pile-up corrected, summed, and fit with the new gates, and half-lives of $T_{1/2} = 70.6234 \pm 0.0859$ s and $T_{1/2} = 70.6367 \pm 0.0854$ s were found. To be conservative, half of the difference between these two values was taken as an additional source of systematic error associated with the $\gamma$-ray gate choice. When added in quadrature with the adopted systematic error arising from the proton beam current grouping of the data, a total systematic error of $\pm 0.037$ s was adopted.

As a final check, the half-life of the $^{26}$Na contaminant was allowed to vary within its $\pm 1\sigma$ limits and the summed (global) fit was repeated. The contribution to the uncertainty in the $^{14}$O half-life was at the level of $<10^{-6}$ and thus completely

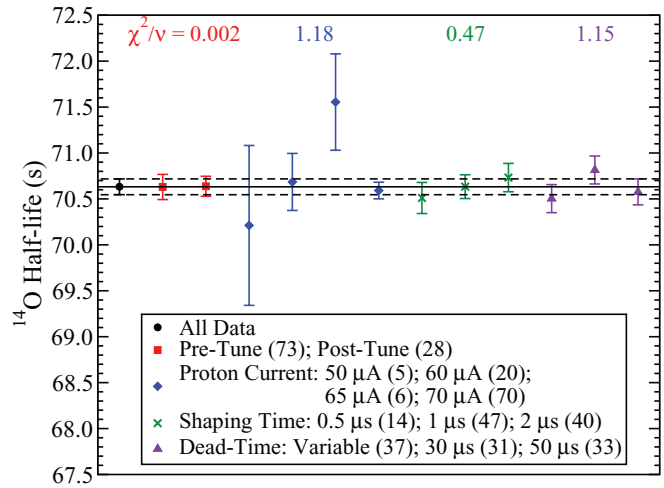


FIG. 9. (Color online) Half-life measurements of $^{14}$O by the $\gamma$-ray technique grouped according to experimental parameters. The numbers in parentheses indicate the number of runs corresponding to each setting. See text for details.

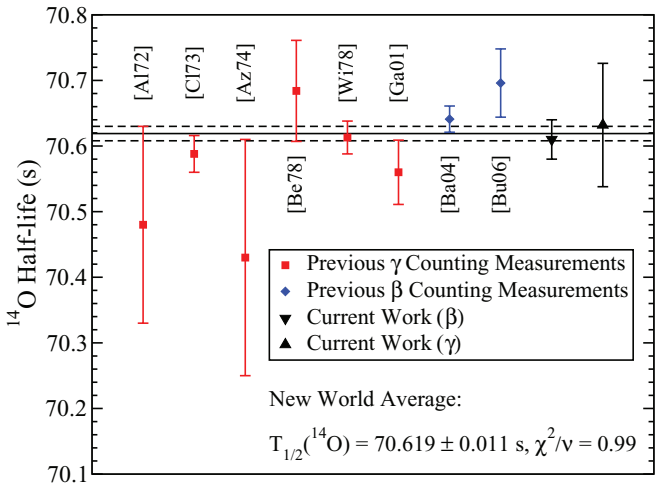


FIG. 10. (Color online) Comparison of the previous $^{14}$O half-life measurements with the current results. References to previous measurements are Al72 [28], Cl73 [29], Az74 [30], Be78 [31], Wi78 [32], Ga01 [33], Ba04 [13], and Bu06 [14], respectively. The new world average $T_{1/2} = 70.619 \pm 0.011$ s, obtained from a weighted average of these results including the current measurements, is overlaid for comparison.

negligible when added in quadrature with the other systematic contributions.

Assuming the statistical and systematic uncertainties are independent quantities and can be combined in quadrature to obtain the overall uncertainty, the half-life of $^{14}$O determined from $\gamma$-ray counting in this work is $T_{1/2}(\gamma) = 70.632 \pm 0.086_{\text{stat.}} \pm 0.037_{\text{syst.}}$ s, entirely consistent with the simultaneous, but independent, $\beta$ counting half-life measurement of $T_{1/2}(\beta) = 70.610 \pm 0.030$ s reported in Sec. III. By combining these results with the eight previous measurements, the world average $^{14}$O half-life becomes $T_{1/2} = 70.619 \pm 0.011$ s with a reduced $\chi^2$ value of 0.99, as presented in Fig. 10.

When reexamining the data based on the detection method used, including the current data, those experiments detecting the 2312.6-keV $\gamma$ rays yield an average value of $T_{1/2}(\gamma) = 70.599(17)$ s while the direct $\beta$ counting measurements yield $T_{1/2}(\beta) = 70.637(16)$ s, results that have a $\chi^2/\nu = 2.83$ if considered as two independent techniques for the measurement of the same quantity, compared to $\chi^2/\nu = 3.85$ when the current data are not included.

## V. CONCLUSIONS

Two simultaneous, but independent, high-precision half-life measurements for the superallowed Fermi $\beta^+$ emitter $^{14}$O were performed, yielding results of $T_{1/2}(\beta) = 70.610 \pm 0.030$ s and $T_{1/2}(\gamma) = 70.632 \pm 0.094$ s.

These results improve the precision of the new world average for the $^{14}$O half-life and also now yield a consistent world data set with $\chi^2/\nu = 0.99$, thereby reducing the uncertainty in the world average from $T_{1/2}(^{14}O) = 70.620 \pm 0.015$ s adopted in Ref. [1] to $T_{1/2}(^{14}O) = 70.619 \pm 0.011$ s.

## ACKNOWLEDGMENTS

This work was partially supported by the Natural Sciences and Engineering Research Council of Canada. TRIUMF receives federal funding via a contribution agreement through the National Research Council of Canada.

[1] J. C. Hardy and I. S. Towner, Phys. Rev. C **79**, 055502 (2009).
[2] I. S. Towner and J. C. Hardy, Rep. Prog. Phys. **73**, 046301 (2010).
[3] J. C. Hardy and I. S. Towner, Phys. Rev. C **71**, 055501 (2005).
[4] N. R. Tolich, P. H. Barker, P. D. Harty, and P. A. Amundsen, Phys. Rev. C **67**, 035503 (2003).
[5] J. Dilling *et al.*, Int. J. Mass Spectrom. **251**, 198 (2006).
[6] R. Sherr, J. B. Gerhart, H. Horie, and W. F. Hornyak, Phys. Rev. **100**, 1024 (1955).
[7] G. Frick, A. Gallmann, D. E. Alburger, D. H. Wilkinson, and J. P. Coffin, Phys. Rev. **132**, 2169 (1963).
[8] G. S. Sidhu and J. B. Gerhart, Phys. Rev. **148**, 1024 (1966).
[9] I. S. Towner and J. C. Hardy, Phys. Rev. C **72**, 055501 (2005).
[10] J. C. Hardy and I. S. Towner, J. Phys.: Conf. Ser. **387**, 012006 (2012).
[11] B. Blank (private communication).
[12] I. S. Towner and J. C. Hardy, Phys. Rev. C **66**, 035501 (2002).
[13] P. H. Barker, I. C. Barnett, G. J. Baxter, and A. P. Byrne, Phys. Rev. C **70**, 024302 (2004).
[14] J. T. Burke, P. A. Vetter, S. J. Freedman, B. K. Fujikawa, and W. T. Winter, Phys. Rev. C **74**, 025501 (2006).
[15] C. E. Svensson *et al.*, Nucl. Instrum. Methods B **204**, 660 (2003).
[16] G. C. Ball *et al.*, J. Phys. G **31**, S1491 (2005).
[17] G. F. Grinyer *et al.*, Nucl. Instrum. Methods A **579**, 1005 (2007).
[18] G. F. Grinyer *et al.*, Phys. Rev. C **71**, 044309 (2005).
[19] P. Finlay *et al.*, Phys. Rev. Lett. **106**, 032501 (2011).
[20] V. T. Koslowsky, E. Hagberg, J. C. Hardy, G. Savard, H. Schmeing, K. S. Sharma, and X. J. Sun, Nucl. Instrum. Methods A **401**, 289 (1997).
[21] P. M. Endt, Nucl. Phys. A **633**, 1 (1998).
[22] A. P. Baerg, Metrologia **3**, 131 (1965).
[23] Particle Data Group, J. Beringer *et al.*, Phys. Rev. D **86**, 010001 (2012).
[24] F. Ajzenberg-Selove, Nucl. Phys. A **523**, 1 (1991).
[25] G. F. Grinyer *et al.*, Phys. Rev. C **76**, 025503 (2007).
[26] G. F. Grinyer *et al.*, Phys. Rev. C **87**, 045502 (2013).
[27] P. Finlay *et al.*, Phys. Rev. C **85**, 055501 (2012).
[28] D. E. Alburger, Phys. Rev. C **5**, 274 (1972).
[29] G. J. Clark, J. M. Freeman, D. C. Robinson, J. S. Ryder, W. E. Burcham, and G. T. A. Squier, Nucl. Phys. A **215**, 429 (1973).
[30] G. Azuelos, J. E. Crawford, and J. E. Kitching, Phys. Rev. C **9**, 1213 (1974).
[31] J. A. Becker, R. A. Chalmers, B. A. Watson, and D. H. Wilkinson, Nucl. Instrum. Methods **155**, 211 (1978).
[32] D. H. Wilkinson, A. Gallmann, and D. E. Alburger, Phys. Rev. C **18**, 401 (1978).
[33] M. Gaelens *et al.*, Eur. Phys. J. A **11**, 413 (2001).